The Effect of the Accommodation Coefficient on Slider Air Bearing Simulation

Weidong Huang and David B. Bogy
Computer Mechanics Laboratory
University of California, at Berkeley

ABSTRACT

In solving the slider air bearing problem, both the Molecular Gas-film Lubrication (MGL) model and the Direct Simulation Monte Carlo (DSMC) model require the accommodation coefficient as input. The accommodation coefficient represents the fraction of the air molecules that interact with solid boundaries in a diffusive manner. In general, the value one is used for the accommodation coefficient, which represents a fully diffusive reflection. However, in magnetic hard disk drives, the disk and slider surfaces are becoming ever smoother with different kinds of lubrication on the disk, while the temperature is becoming higher due to the faster spindle speed. Under these conditions the unit value of the accommodation coefficient may no longer be suitable. In order to understand the effect of the accommodation coefficient on the slider's flying parameters, we used Kang's new database for the Poiseuille flow rate Q_p and Couette flow rate Q_c to solve the modified Reynolds equation for two groups of sliders, e.g., negative and positive pressure sliders ("negative" refers to sliders with sub-ambient pressure zones). The results show that, in general, the smaller the accommodation coefficient, the lower the flying height and pitch angle. Positive pressure sliders are more sensitive to the accommodation coefficient than are negative pressure sliders. The typical discrepancy in flying height is around 10%. Also, it is shown that for positive pressure sliders the lower the flying height, the larger the discrepancy percentage.

1. INTRODUCTION

In a modern Winchester-type disk drive, the read/write element is attached to a slider that flies over a spinning disk. To increase the areal density, the slider is designed to fly microscopically close ($h < 50$ nm) to the moving disk surface. Since the minimum clearance between the slider and the disk is close to or even less than the mean free path of the air molecules (65 nm at STP), the flow may not satisfy the non-slip condition at the solid boundaries. The conventional compressible lubrication equations are not valid in this situation.

The widely used Molecular Gas-film Lubrication (MGL) model (Fukui and Kaneko, 1988) is the Reynolds equation with the slip correction based on Boltzmann's equation, where the Poiseuille flow rate is calculated on the basis of a linearized BGK model of the Boltzmann equation. The MGL model was verified for flying heights down to a couple of nanometers by a series of studies using the particle-based Direct Simulation Monte Carlo Method (DSMC). It has been shown that the two models predict results that are in good agreement (Alexander, et. al. 1994, Huang, et. al., 1997). This assures that the MGL model based air bearing simulator is a reliable tool for designing sliders flying well under 25 nm.

In both the MGL model and the DSMC model, the gas-surface accommodation coefficient, denoted by α, is required as input. Fukui and Kaneko (1990) obtained a database for the Poiseuille flow rate Q_p with different accommodation coefficients ranging from 0.7 to 1. In their modeling they considered only the cases when the slider and the disk have the same accommodation coefficient. When there is a difference between the accommodation coefficients of the slider and the disk, the Couette flow term in the modified Reynolds equation also has to be corrected because of the loss of symmetric of the velocity profile. When the slider and disk have different

accommodation coefficients, in the range from 0.7 to 1, Kang et al. (1997) obtained both the Poiseuille flow rate and the Couette flow rate coefficients. In addition, they found that Fukui and Kaneko's database contained a numerical error in Q_p for small Knudsen numbers when the accommodation coefficient is not unity. They made the corrections in their new database.

There is very limited published information on the value of the accommodation coefficient to be used when solving the air bearing problem for the head disk interface (HDI). Kennard (1938) listed the accommodation coefficient for a number of cases obtained by other researchers. The cases listed there are not directly relevant to the current HDI. Rettner (1997) used molecular beam techniques to obtain the accommodation coefficient for N_2 colliding with a sputtered carbon overcoat and a lubricated Pt(111) surface, as well as sections of a glass disk used in fly-height testing and of an actual 3.5-in disk. The temperatures of the surfaces were either 0 °C or 20 °C. Wenski et al. (1998) used a linear fit of Rettner's data to obtain the accommodation coefficient for N_2 at room temperature. They concluded that the accommodation coefficient was around 0.95 when both N_2 and the four surfaces studied by Rettner were at room temperature.

Due to the absence of a complete database of accommodation coefficients for the current HDI, most slider designers use complete thermal accommodation, i.e. $\alpha = 1$. But many researchers have pointed out that the accommodation coefficient varies with different surface materials, temperatures and surface roughness (Kennard, 1937, Bird, 1994, Wadsworth, 1993, Kang, 1997).

In a typical HDI, α for the slider is normally greater or equal to α for the disk (Kang, 1997). This is due to the fact that the lubricated disk surface is smoother than the carbon-over-coated slider surface (In general, the accommodation coefficient is smaller for a smoother surface.).

As sliders fly lower and lower, the simulations are required to be increasingly more accurate. The effect of the accommodation coefficient α on the slider air bearing design needs to be

understood. In this paper, we implement Kang's (1997) database for the Poiseuille flow rate coefficient and the Couette flow rate coefficient with the accommodation coefficients in the range from 0.7 to 1 in the CML Slider Air Bearing Design Program (Lu, et al. 1997). Simulations of several negative and positive pressure sliders are carried out, and the results for the flying height and the pitch angle are compared to the cases of unity accommodation coefficient.

2. ACCOMMODATION COEFFICIENT

In rarefied gas flow simulations, one of the major problems is modeling the interaction of gas molecules with solid surfaces. The accommodation coefficient expresses the tendency of the gas to accommodate to the state of the wall. The commonly used accommodation coefficient was introduced by Knudsen in 1911 (Kennard, 1938). In terms of energy, the accommodation coefficient can be defined by:

$$\alpha = (E_i - E_r) / (E_i - E_w) \tag{1}$$

where E_i denotes the energy rate per unit area of the incident molecules, E_r denotes the energy carried away by the reflected molecules and E_w denotes the energy that would be carried away by the reflected molecules in diffuse reflection at the wall temperature.

In an appendix to a paper published in the Philosophical Transactions of the Royal Society in 1879, Maxwell proposed two models for the interaction of an equilibrium gas with a solid surface that maintained equilibrium:

1. The first model was that of perfectly specular reflection, which is an elastic model, with the molecular velocity component normal to the surface being reversed while those parallel to the surface remain unchanged. The gas cannot exert any stress on the surface except in the normal direction of the wall. In this case, $E_r = E_i$. According to eq. (1), α is then equal to zero.
2. The second model was that of perfectly diffusive reflection. The incident molecules have their mean energy and momentum adjusted or "accommodated" and then re-evaporate at the temperature of the surface. In this case, $E_r = E_w$ and α is equal to one as determined by eq. (1).

Since the above two idealized models cannot be used to represent gas interaction with actual physical surfaces, Maxwell assumed a gas-solid interaction that is intermediate between them. He assumed that a fraction φ of the molecules are diffusively reflected with accommodation

coefficient $\alpha_{dif} = 1$ and the rest are specularly reflected with accommodation coefficient $\alpha_{spe} = 0$. Then the energy reflected will be:

$$E_r = \varphi * E_w + (1 - \varphi) * E_i \tag{2}$$

This leads to

$$\alpha = \varphi \tag{3}$$

So Maxwell's accommodation coefficient (in terms of energy or momentum) represents the fraction of molecules that experience diffusive reflection from the solid surface.

However, Cercignani (1969) pointed out that in physical interactions, momentum is lost or gained much faster than energy. This reveals a basic inaccuracy of Maxwell's boundary conditions. That is, the distribution function obtained from the momentum accommodation boundary condition does not necessarily give correct phenomenological results for energy accommodation. Further studies have shown that stochastic models for the boundary conditions define a probability distribution function for the velocity (Goodman and Wachman, 1976). Cercignani (1972) showed that this distribution should satisfy a reciprocity (or detailed balance) condition. Cercignani and Lampis (1971) derived a realistic distribution that satisfied reciprocity.

Nevertheless, due to its simplicity and reasonable accuracy, Maxwell's boundary conditions are frequently used by many researchers, including Fukui and Kaneko (1988), Huang, et al. (1997) and Kang, et al. (1997). In this study, we will follow their approach and adopt the same accommodation coefficient α for the boundary condition.

3. MODIFIED REYNOLDS EQUATION

When the Couette flow rate coefficient is considered for the air bearing problem in the HDI, the two-dimensional steady state generalized Reynolds equation is given by (See Kang, 1997):

$$\frac{\partial}{\partial X}(Q_p PH^3 \frac{\partial P}{\partial X} - \Lambda_x Q_c PH) + \frac{\partial}{\partial Y}(Q_p PH^3 \frac{\partial P}{\partial Y} - \Lambda_y Q_c PH) = 0 \qquad (4)$$

where $P = p / p_a$, $H = h / h_m$, $X = x / L$, $Y = y / L$ are the non-dimensionalized pressure, bearing clearance or flying height, coordinate in the slider length direction and coordinate in the slider width direction, respectively; p_a is the ambient atmospheric pressure; h_m is the reference clearance at the trailing edge center; L is the length of the slider; Λ_x and Λ_y are the bearing numbers in the x and y directions, respectively; Q_p and Q_c are the Poiseuille and Couette flow rate coefficients, respectively. Both of which are given in Kang's database. For convenience, define $\Delta\alpha$ by:

$$\Delta\alpha = \alpha_1 - \alpha_0$$

where α_1 is the accommodation coefficient at the slider and α_0 is the accommodation coefficient at the disk. Due to the reasons mentioned at Sec. 1, Q_p and Q_c are obtained by Kang only for the cases with $\Delta\alpha \geq 0$. In addition, we used an interpolation to obtain the values $Q_c(\alpha_0, \alpha_1)$ that are not available in Kang's database. For example, Kang's database does not have $Q_c(0.85, 0.9)$. We used $Q_c(0.90, 0.90)$, $Q_c(0.80, 0.90)$, $Q_c(0.85, 0.95)$, $Q_c(0.85, 0.85)$ to obtain $Q_c(0.85, 0.9)$ from the following formula:

$$Q_c(0.85,0.90) = \frac{1}{2}\left\{\frac{1}{2}\left[Q_c(0.85,0.85) + Q_c(0.85,0.95)\right] + \frac{1}{2}\left[Q_c(0.80,0.90) + Q_c(0.90,0.90)\right]\right\} \qquad (5)$$

To solve for the Reynolds equation, we used the CML Air Bearing Design Program (version 418) with the following modifications. We

(i) Changed the Q_p database from Fukui-Kaneko's to Kang's when $\Delta\alpha \neq 0$;

(ii) Added the Q_c database obtained by Kang into the Reynolds equation solver.

(iii) Added Q_c into the Couette flow term in the modified Reynolds equation. When $\Delta\alpha = 0$, Q_c is unity. Otherwise, the program will use the Q_c table for the local Knudsen number.

(iv) Added the values of α_0 and α_1 into the **run.dat** file.

4. SIMULATION RESULTS

Base on the discussion in Sec. 1, we can assume that α falls into the range from 0.90 to 1 for most cases in the HDI. In this report, we allow α_0 and α_1 to independently take the values 0.85, 0.9, 0.95 and 1. The sliders we used are divided into two categories: negative pressure sliders and positive pressure sliders. For the negative ones, we have chosen the NSIC "Nutcracker", Headway AAB and TFN (Taper Flat Negative, Garniew et al., 1974; Kogure et al., 1993; White, 1983) sliders. For the positive ones, we have chosen the TPC (Transverse Pressure Contour, White, 1991), TF (Taper Flat) and Read-Rite Tri-Pad sliders. The rail shapes of the sliders used are plotted in Figs. 1 and 2. All sliders are the so-called 50% sliders, i.e. 2.0 mm in length, 1.6 mm in width and 0.42 mm in height. The radial position of the sliders in all simulations is at 30 mm with no skew angle. The suspension loading force is 3.5 gram. The ambient pressure and viscosity are 1.014×10^5 Pa and 1.806×10^{-5} Nsm-2. The number of grids used in the simulations is 197x197. All flying heights presented in this report are for the point at the read/write element.

First, we considered the TPC slider. The point of interest is at (x, y) = (1.999 mm, 1.350 mm). The spindle speed is 5,400 rpm. The designation of this TPC slider is TPC_100, and it is used to compare to other TPC sliders with different rail widths. The flying height at the point of interest in nanometers is tabulated in Table 1(a) as a function of (α_0, α_1). Adjacent to the flying height, we also list the relative difference ε between the flying height at various (α_0, α_1) and the one at $\alpha_0 = \alpha_1 = 1$, i. e.

$$\varepsilon = \frac{[H(\alpha_0, \alpha_1) - H(1,1)]}{H(1,1)} \tag{6}$$

We did not calculate the cases when $\alpha_0 > \alpha_1$ due to the fact that Q_c is not available in Kang's (1997) database (see Sec. 1). It can be seen that the flying height decreases when either α_0 or α_1 gets

smaller. For the data on the diagonal, there is no Couette flow correction since the flow symmetry is retained in those cases. Then only the Poiseuille flow rate coefficient is corrected. The effect of this correction changes the flying height by -4.5% to -13.5%.

Consider the change for a point on the diagonal of the table, for example, ε (0.95,0.95) = -4.5%. It can be seen that when α_0 is decreased by 0.5, ε (0.90, 0.95) = -7.3%. On the other hand, when α_1 is increased by 0.5, ε (0.95, 1) = -2.9%. These two trends are also seen from other data presented in this report. This shows that the Couette flow correction has two effects, depending on how the flow deviates from the symmetric case. When the deviation is caused by decreasing the disk accommodation coefficient, the relative discrepancy is larger. When it is caused by increasing the head accommodation coefficient, it is smaller.

Next, we changed the air bearing surface area of the TPC_100 slider and created two other TPC sliders, one has 75% of the original TPC slider air bearing surface area and is designated TPC_75, the other one, TPC_60, has a 60% area. These two sliders fly lower than the original one due to the smaller air bearing surface. After calculating their flying heights with different accommodation coefficients, we tabulated the data in the same fashion in Table 1(b) and 1(c). In this manner, we investigated the effect of the accommodation coefficient on the flying height when these TPC sliders fly at different altitudes. Comparing the data from Table 1(a) with that in Table 1(b) and 1(c), for example, when (α_0, α_1) = (0.90, 0.95), we find the following. The data in the three tables are 89.49 (-7.3%), 38.99 (-9.1%) and 14.27 (-11.5%). Therefore the magnitude of ε increases when the flying height decreases. This is true for each pair of α in Table 1.

In another test, we used the TPC_75 slider and changed the flying height by changing the spindle speed from 5,400 rpm in the simulation to 7,200 rpm and then to 10,000 rpm. The resulting

data are tabulated in Table 2(a-c). Again, we notice that $|\varepsilon|$ increases when the flying height decreases.

However, these trends do not hold for all sliders. Table 3 lists the simulation results for the NSIC "Nutcracker" slider at three rpm values; 5,400, 7,200 and 10,000. Comparing the data for these three cases, we find that the larger the flying height, the larger the magnitude of ε. This is different from what was observed for the TPC slider. It also can be seen that by comparing cases with the same (α_0, α_1), the discrepancy caused by the accommodation coefficient is larger for the TPC slider than for the "Nutcracker" slider.

In order to make a more comprehensive comparison, we simulated several other sliders with variations of the accommodation coefficient and the flying height. The sliders considered were the Headway AAB, TFN, TF, TF_modf and the Tri-Pad slider.

TF_modf represents the TF slider modified so that it has the same reference flying height h_m and the pitch angle as the "Nutcracker" slider. Otherwise the TF slider has very different designed flying height and flying attitude from the "Nutcracker" slider and a valid comparison is not possible.

The modified rail shape is shown in Fig. 3. The reference flying height is about 32 nm and the pitch angle is about 190 μrad, which are very similar to the "Nutcracker" slider. The simulation results are presented in Table 4. Comparing Table 4 with Table 3, we see that the discrepancy for the modified TF slider is larger than that for the "Nutcracker" slider, even though their flying attitudes are similar.

The results for the Headway AAB, TFN, TF, and the Tri-Pad slider are tabulated in Table 5 through Table 8, respectively. From them we conclude that the positive pressure sliders have larger deviations from the results with unity accommodation coefficient than the negative pressure sliders.

In addition, the TF_modf slider is designed to fly lower than the original TF slider. It can be seen from Tables 4 and 7 that, as the other positive pressure sliders showed, the lower the flying height, the larger the deviation from the results with unity accommodation coefficient.

In order to illustrate the effect more clearly we picked one pair of data, i.e. the flying height H and its relative discrepancy ε from each table with the same (α_0, α_1) and plotted it in Fig. 4. The data in Fig. 4(a) are for $\alpha_0 = 0.95$, $\alpha_1 = 1$. The data in Fig. 4(b) are for $\alpha_0 = 0.90$, $\alpha_1 = 0.95$ and the data in Fig. 4(c) are for $\alpha_0 = 0.90$, $\alpha_1 = 0.90$. There are eight sets of data for the various sliders presented in Fig. 4. Among them, only the TPC_% represents a case for which the change of the flying height is due to the change of the air bearing surface area.

Figure 4 clearly shows that the positive pressure sliders follow a trend; the lower the slider flies, the greater the effect caused by the various accommodation coefficients. But the negative pressure sliders behave differently. The "Nutcracker" slider shows that the deviation is larger for higher flying heights. The TFN slider shows the opposite, which matches the positive pressure sliders. The flying height of the Headway AAB slider falls into a very small interval from about 22 nm to 24 nm due to its insensitivity to the disk velocity. In Fig. 4(a) and 4(b), this slider shows decreasing trends while in Fig. 4(c), it has an increasing curve.

From Figure 4, one can also conclude that the positive pressure sliders tend to have a larger ε than the negative pressure sliders in the flying height range from 20 nm to 60 nm. Again, the three figures together show that when the accommodation coefficients decrease, ε becomes larger.

Among the parameters of interest in slider air bearing design, pitch angle is especially important. The effect of the accommodation coefficient on the pitch angle is also studied. The

results from the “Nutcracker” slider, TF slider and the modified TF slider are presented. The other sliders have similar behavior.

Tables 9 ~ 11 show the pitch angle results for these three sliders. Their percent differences from the cases in which the accommodation coefficients are one are much smaller than for the flying height. The positive pressure slider TF has a slightly larger difference than the “Nutcracker” slider, while the modified TF slider, which has similar flying attitude to the “Nutcracker” slider, has almost the same discrepancy as the “Nutcracker” slider.

5. CONCLUSIONS

A numerical study was conducted to investigate the effect of the accommodation coefficient on slider flying height by using a modified CML Air Bearing Design Program. Both positive and negative pressure sliders were chosen for comparison with each other. The accommodation coefficients ranged from 0.85 to 1 with increments of 0.5. The simulation results show the following:

1) The non-unity accommodation coefficients lower the flying height. This includes two cases:
   (a) When the accommodation coefficients for the disk and the slider are the same, the Couette flow rate coefficient is one. Only the Poiseuille flow rate coefficient is modified. This change leads to lower flying height, up to about 10% difference from the case when the accommodation coefficient is unity.
   (b) When the disk has a different accommodation coefficient than the slider, both the Poiseuille and Couette flow rate coefficients have to be corrected. The resulting effect depends on how the case is biased from the symmetric case, i.e. the case discussed in (a). If it is biased due to increasing the slider's accommodation coefficient, the flying height is increased. If it is biased due to decreasing the disk's accommodation coefficient, the flying height is decreased.
2) The positive pressure sliders are more sensitive to the variation of the accommodation coefficient than the negative pressure sliders.
3) For the positive pressure sliders, the lower they fly, the more sensitive they are to the variation of the accommodation coefficient. However, different negative pressure sliders show a different behavior in this case.

4) The pitch angle is not as sensitive to the accommodation coefficient as the flying height, percentage wise.

The CML Air Bearing Design Code is being modified to include the newly published Q_p and Q_c database, which should, in principal, allow the computation of more accurate results. Especially for those who want to know the effect of different lubricants on the slider air bearings, the improved simulator may be more useful. However, we make no recommendation as to what values to use for the accommodation coefficients.

6. REFERENCE

Alexander, F. J., Garcia, A. L. and Alder, B. J., “Direct Simulation Monte Carlo for thin-film bearings,” Phys. Fluids, Vol. 6, pp. 3854-3860, 1994.

Bird, G. A., *Molecular Gas Dynamics and the Direct Simulation of Gas Flows*, Clarendon, Oxford, 1994.

Cercignani, C., *Mathematical Methods in Kinetic Theory*, Plenum Press Inc., New York, 1969.

Cercignani, C. and Lampis, M., “Kinetic Models for Gas-Surface Interactions,” *Trans. Th. and Stat. Phys.*, Vol. 1, pp. 101-114.

Cercignani, C., “Scattering Kernels for Gas-Surface Interactions,” *Trans. Th. and Stat. Phys.*, Vol. 2, pp. 27-53.

Fukui, S. and Kaneko, R., "Analysis of Ultra-Thin Gas Film Lubrication Based on Linearized Boltzmann Equation: First Report - Derivation of a Generalized Lubrication Equation Including Thermal Creep Flow," ASME J. of Tribology 110, 253, 1988.

Fukui, S. and Kaneko, R., "A Database for Interpolation of Poiseuille Flow Rates for High Knudsen Number Lubrication Problems," ASME J. of Tribology 112, 78, 1990

Garnier, M. F., Tang, T. and White, J. W., “Magnetic Head Slider Assembly,” U.S. Patent No. 3855625, 1974.

Goodman, F. O. and Wachman, H. Y., Dynamics of Gas-Surface Scattering, Academic Press, New York, 1976.

Huang, W., Bogy, D. B., and Garcia, A. L., “Three-Dimensional Direct Simulation Monte Carlo Method for Slider Air Bearings,” Phys. Fluids, Vol. 9, pp. 1764-1769, 1997.

Kang, S.-C., Jhon, M. S. and Crone, R. M., "Corrections to and Extensions of the Molecular Gas Lubrication Theory," Proceedings of the International Conference on Micromechatronics for Information and Precision Equipment, Japan, 1997

Kang, S.-C., "A Kinetic Theory Description for Molecular Lubrication," Ph.D. Thesis, Carnegie Mellon University, 1997.

Kennard, E. H., *Kinetic Theory of Gases with an Introduction to Statistical Mechanics*, McGraw-Hill, New York, NY, 1938

Kogure K., Fukui S., Mitsuya Y. and Kaneko R., 1993, “Design of Negative Pressure Slider for Magnetic Recording Disks,” ASME, J. of Lubrication Technology, Vol. 105, pp. 496-502, 1993.

Lu, S., “Numerical Simulation of Slider Air Bearings,” Ph.D. Thesis, University of California at Berkeley, 1997.

Maxwell, J. C., Phil. Trans. R. Soc. I, Appendix, 1879; reprinted in*: The Scientific Papers of J. C. Maxwell*, Dover Publications, 1965.

Rettner, C., “Determination of Accommodation Coefficients for N_2 at Disk-Drive Air-Bearing Surfaces,” J. Tribology, Vol. 119, pp. 588-589, 1997.

Wadsworth, D. C., “Slip Effects in a Confined Rarefied Gas. I: Temperature Slip, ” Phys. Fluids, **10**, 332, 1967.

White, J. W., “The Transverse Pressure Contour Slider: Flying Characteristics and Comparison with Taper-Flat and Cross-Cut Type Sliders,” ASME, Adv. in Info. Storage Syst., Vol. 3, pp. 1-14, 1991.

White, J. W., “Flying Characteristics of the ‘Zero-Load’ Slider Bearing,*” J. of Lubrication Technology*, Vol. 105, pp. 484-490, 1983.

TABLE 1. Effect of the Flying Height for the TPC Sliders

(a)

TPC_100		Accommodation Coefficient for the Slider, α_1			
		1.00	0.95	0.90	0.85
Accommodation coefficient for the disk, α_0	1.00	96.5421	-	-	-
	0.95	93.7723 (-2.9%)	92.2047 (-4.5%)	-	-
	0.90	90.9570 (-5.8%)	89.4895 (-7.3%)	87.9162 (-8.9%)	-
	0.85	88.0826 (-8.8%)	86.5603 (-10.3%)	84.9260 (-12.0%)	83.4720 (-13.5%)

(b)

TPC_75		Accommodation Coefficient for the Slider, α_1			
		1.00	0.95	0.90	0.85
Accommodation coefficient for the disk, α_0	1.00	42.9143	-	-	-
	0.95	41.2707 (-3.8%)	40.6306 (-5.3%)	-	-
	0.90	39.7564 (-7.4%)	38.9888 (-9.1%)	38.4273 (-10.5%)	-
	0.85	38.0361 (-11.4%)	37.4198 (-12.8%)	36.7457 (-14.4%)	36.1412 (-15.8%)

(c)

TPC_60		Accommodation Coefficient for the Slider, α_1			
		1.00	0.95	0.90	0.85
Accommodation coefficient for the disk, α_0	1.00	16.1178	-	-	-
	0.95	15.1531 (-6.0%)	15.2716 (-5.3%)	-	-
	0.90	14.4297 (-10.5%)	14.2699 (-11.5%)	14.1225 (-12.4%)	-
	0.85	13.6416 (-15.4%)	13.5411 (-16.0%)	13.3979 (-16.9%)	13.2915 (-17.5%)

TABLE 2. Effect of the Flying Height for the TPC_75 Sliders

(a)

TPC_75 RPM = 5,400		Accommodation Coefficient for the Slider, α_1			
		1.00	0.95	0.90	0.85
Accommodation coefficient for the disk, α_0	1.00	42.9143	-	-	-
	0.95	41.2707 (-3.8%)	40.6306 (-5.3%)	-	-
	0.90	39.7564 (-7.4%)	38.9888 (-9.1%)	38.4273 (-10.5%)	-
	0.85	38.0361 (-11.4%)	37.4198 (-12.8%)	36.7457 (-14.4%)	36.1412 (-15.8%)

(b)

TPC_75 RPM = 7,200		Accommodation Coefficient for the Slider, α_1			
		1.00	0.95	0.90	0.85
Accommodation coefficient for the disk, α_0	1.00	57.5519	-	-	-
	0.95	55.5610 (-3.5%)	54.5984 (-5.1%)	-	-
	0.90	53.5192 (-7.0%)	52.6197 (-8.6%)	51.6865 (-10.2%)	-
	0.85	51.4674 (-10.6%)	50.5490 (-12.2%)	49.5444 (-13.9%)	48.6947 (-15.4%)

(c)

TPC_75 RPM = 10,000		Accommodation Coefficient for the Slider, α_1			
		1.00	0.95	0.90	0.85
Accommodation coefficient for the disk, α_0	1.00	83.4876	-	-	-
	0.95	80.8782 (-3.1%)	79.3146 (-5.0%)	-	-
	0.90	78.1215 (-6.4%)	76.7546 (-8.1%)	75.3681 (-9.7%)	-
	0.85	75.4363 (-9.6%)	74.0638 (-11.3%)	72.5194 (-13.1%)	71.1951 (-14.7%)

TABLE 3. Effect of the Flying Height for the "Nutcracker" Sliders

(a)

"Nutcracker" RPM = 5,400		Accommodation Coefficient for the Slider, α_1			
		1.00	0.95	0.90	0.85
Accommodation coefficient for the disk, α_0	1.00	22.5512	-	-	-
	0.95	22.3100 (-1.1%)	21.6831 (-3.8%)	-	-
	0.90	22.2727 (-1.2%)	21.2166 (-5.9%)	20.9417 (-7.1%)	-
	0.85	21.8961 (-2.9%)	21.0195 (-6.8%)	20.2546 (-10.2%)	19.7489 (-12.4%)

(b)

"Nutcracker" RPM = 7,200		Accommodation Coefficient for the Slider, α_1			
		1.00	0.95	0.90	0.85
Accommodation coefficient for the disk, α_0	1.00	26.6048	-	-	-
	0.95	26.0899 (-1.9%)	25.2192 (-5.2%)	-	-
	0.90	25.7842 (-3.0%)	25.0066 (-6.0%)	24.1377 (-9.3%)	-
	0.85	25.7425 (-3.2%)	24.8783 (-6.5%)	23.8598 (-10.3%)	22.9242 (-13.8%)

(c)

"Nutcracker" RPM = 10,000		Accommodation Coefficient for the Slider, α_1			
		1.00	0.95	0.90	0.85
Accommodation coefficient for the disk, α_0	1.00	37.9300	-	-	-
	0.95	36.9783 (-2.5%)	35.8689 (-5.4%)	-	-
	0.90	36.4085 (-4.0%)	35.3444 (-6.8%)	34.2052 (-9.8%)	-
	0.85	36.1633 (-4.7%)	34.9829 (-7.8%)	33.7040 (-11.1%)	32.4885 (-14.4%)

TABLE 4. Flying Height Comparison for the Modified TF Sliders

(a)

TF_modf RPM = 5,400		Accommodation Coefficient for the Slider, α_1			
		1.00	0.95	0.90	0.85
Accommodation coefficient for the disk, α_0	1.00	31.5020	-	-	-
	0.95	30.1988 (-4.1%)	29.3964 (-6.7%)	-	-
	0.90	28.8950 (-8.3%)	28.2340 (-10.4%)	27.4850 (-12.8%)	-
	0.85	27.4701 (-12.8%)	26.7544 (-15.1%)	26.1060 (-17.1%)	25.5126 (-19.0%)

(b)

TF_modf RPM = 7,200		Accommodation Coefficient for the Slider, α_1			
		1.00	0.95	0.90	0.85
Accommodation coefficient for the disk, α_0	1.00	40.8706	-	-	-
	0.95	39.3226 (-3.8%)	38.4740 (-5.9%)	-	-
	0.90	37.9100 (-7.2%)	37.0268 (-9.4%)	36.1885 (-11.5%)	-
	0.85	36.2628 (-11.3%)	35.4557 (-13.3%)	34.5565 (-15.5%)	33.5701 (-17.9%)

(c)

TF_modf RPM = 10,000		Accommodation Coefficient for the Slider, α_1			
		1.00	0.95	0.90	0.85
Accommodation coefficient for the disk, α_0	1.00	53.3942	-	-	-
	0.95	51.5622 (-3.4%)	50.4468 (-5.5%)	-	-
	0.90	49.8907 (-6.6%)	48.7392 (-8.7%)	47.6244 (-10.8%)	-
	0.85	47.9693 (-10.2%)	46.8701 (-12.2%)	45.6965 (-14.4%)	44.3988 (-16.9%)

TABLE 5 Flying Height Comparison for the Headway AAB Sliders

(a)

Headway AAB RPM = 5,400		**Accommodation Coefficient for the Slider, α_1**			
		1.00	0.95	0.90	0.85
Accommodation coefficient for the disk, α_0	1.00	22.2310	-	-	-
	0.95	21.5975 (-2.9%)	21.2493 (-4.4%)	-	-
	0.90	20.9914 (-5.6%)	20.6098 (-7.3%)	20.2746 (-8.8%)	-
	0.85	20.2908 (-8.7%)	19.9154 (-10.4%)	19.6005 (-11.8%)	19.3030 (-13.2%)

(b)

Headway AAB RPM = 7,200		**Accommodation Coefficient for the Slider, α_1**			
		1.00	0.95	0.90	0.85
Accommodation coefficient for the disk, α_0	1.00	22.4964	-	-	-
	0.95	21.8759 (-2.8%)	21.4868 (-4.5%)	-	-
	0.90	21.2830 (-5.4%)	20.8524 (-7.3%)	20.4804 (-9.0%)	-
	0.85	20.5922 (-8.5%)	20.1797 (-10.3%)	19.8043 (-12.0%)	19.4585 (-13.5%)

(c)

Headway AAB RPM = 10,000		**Accommodation Coefficient for the Slider, α_1**			
		1.00	0.95	0.90	0.85
Accommodation coefficient for the disk, α_0	1.00	23.5002	-	-	-
	0.95	22.8885 (-2.6%)	22.4491 (-4.5%)	-	-
	0.90	22.3019 (-5.1%)	21.8128 (-7.2%)	21.3685 (-9.1%)	-
	0.85	21.5839 (-8.2%)	21.1130 (-10.3%)	20.6901 (-12.0%)	20.2837 (-13.7%)

TABLE 6. Flying Height Comparison for the TFN Sliders

(a)

TFN RPM = 5,400		Accommodation Coefficient for the Slider, α_1			
		1.00	0.95	0.90	0.85
Accommodation coefficient for the disk, α_0	1.00	49.2997	-	-	-
	0.95	47.9673 (-2.7%)	47.2599 (-4.1%)	-	-
	0.90	46.6526 (-5.4%)	45.8790 (-6.9%)	45.1645 (-8.4%)	-
	0.85	45.1560 (-8.4%)	44.4087 (-9.9%)	43.6933 (-11.4%)	43.0511 (-12.7%)

(b)

TFN RPM = 7,200		Accommodation Coefficient for the Slider, α_1			
		1.00	0.95	0.90	0.85
Accommodation coefficient for the disk, α_0	1.00	52.2153	-	-	-
	0.95	50.8995 (-2.5%)	50.1666 (-3.9%)	-	-
	0.90	49.7067 (-4.8%)	48.8879 (-6.4%)	48.0949 (-7.9%)	-
	0.85	48.2726 (-7.6%)	47.4432 (-9.1%)	46.6464 (-10.7%)	45.9352 (-12.0%)

(c)

TFN RPM = 10,000		Accommodation Coefficient for the Slider, α_1			
		1.00	0.95	0.90	0.85
Accommodation coefficient for the disk, α_0	1.00	54.8216	-	-	-
	0.95	53.5376 (-2.3%)	52.7270 (-3.8%)	-	-
	0.90	52.4023 (-4.4%)	51.4228 (-6.2%)	50.6019 (-7.7%)	-
	0.85	50.9670 (-7.0%)	50.1014 (-8.6%)	49.2243 (-10.2%)	48.4106 (-11.7%)

TABLE 7. Flying Height Comparison for the TF Sliders

(a)

TF RPM = 5,400		Accommodation Coefficient for the Slider, α_1			
		1.00	0.95	0.90	0.85
Accommodation coefficient for the disk, α_0	1.00	49.4901	-	-	-
	0.95	47.6888 (-3.6%)	46.8411 (-5.4%)	-	-
	0.90	45.8391 (-7.4%)	45.0958 (-8.9%)	44.3200 (-10.5%)	-
	0.85	44.0179 (-11.1%)	43.2540 (-12.6%)	42.4435 (-14.2%)	41.7429 (-15.7%)

(b)

TF RPM = 7,200		Accommodation Coefficient for the Slider, α_1			
		1.00	0.95	0.90	0.85
Accommodation coefficient for the disk, α_0	1.00	69.4784	-	-	-
	0.95	67.3976 (-3.0%)	66.2202 (-4.7%)	-	-
	0.90	65.0928 (-6.3%)	63.9814 (-7.9%)	62.9296 (-9.4%)	-
	0.85	48.2726 (-7.6%)	47.4432 (-9.1%)	46.6464 (-10.7%)	45.9352 (-12.0%)

(c)

TF RPM = 10,000		Accommodation Coefficient for the Slider, α_1			
		1.00	0.95	0.90	0.85
Accommodation coefficient for the disk, α_0	1.00	96.0491	-	-	-
	0.95	93.5423 (-2.6%)	91.9250 (-4.3%)	-	-
	0.90	90.7683 (-5.5%)	89.2962 (-7.0%)	87.7874 (-8.6%)	-
	0.85	88.0291 (-8.3%)	86.4927 (-9.9%)	84.9115 (-11.6%)	83.4655 (-13.1%)

TABLE 8. Flying Height Comparison for the Tri-Pad Sliders

Tri-Pad RPM = 5,400		**Accommodation Coefficient for the Slider, α_1**			
		1.00	0.95	0.90	0.85
Accommodation coefficient for the disk, α_0	1.00	50.5708	-	-	-
	0.95	49.2076 (-2.7%)	47.3724 (-6.3%)	-	-
	0.90	48.0715 (-4.9%)	46.3322 (-8.4%)	44.3535 (-12.3%)	-
	0.85	46.7091 (-7.6%)	45.1427 (-10.7%)	43.1977 (-14.6%)	41.1331 (-18.7%)

TABLE 9. Pitch Angle Comparison for the "Nutcracker" Sliders

"Nutcracker" RPM = 5,400		Accommodation Coefficient for the Slider, α_1			
		1.00	0.95	0.90	0.85
Accommodation coefficient for the disk, α_0	1.00	196.7137	-	-	-
	0.95	193.7424 (-1.5%)	192.5015 (-2.1%)	-	-
	0.90	191.6712 (-2.6%)	190.0845 (-3.4%)	188.0962 (-4.4%)	-
	0.85	189.7596 (-3.5%)	188.2153 (-4.3%)	186.1035 (-5.4%)	183.7363 (-6.6%)

TABLE 10. Pitch Angle Comparison for the TF Sliders

TF RPM = 5,400		Accommodation Coefficient for the Slider, α_1			
		1.00	0.95	0.90	0.85
Accommodation coefficient for the disk, α_0	1.00	70.8372	-	-	-
	0.95	69.6731 (-1.6%)	68.8786 (-2.8%)	-	-
	0.90	68.6203 (-3.1%)	67.6281 (-4.5%)	66.8579 (-5.6%)	-
	0.85	67.4266 (-4.8%)	66.5562 (-6.0%)	65.6011 (-7.4%)	64.7002 (-8.7%)

TABLE 11. Pitch Angle Comparison for the modified TF Sliders

TF_modf RPM = 5,400		Accommodation Coefficient for the Slider, α_1			
		1.00	0.95	0.90	0.85
Accommodation coefficient for the disk, α_0	1.00	199.39	-	-	-
	0.95	196.8632 (-1.5%)	194.8368 (-2.3%)	-	-
	0.90	194.1166 (-2.6%)	192.0445 (-3.7%)	190.4944 (-4.5%)	-
	0.85	191.7530 (-3.8%)	191.3990 (-4.0%)	187.6824 (-5.9%)	185.4444 (-7.0%)

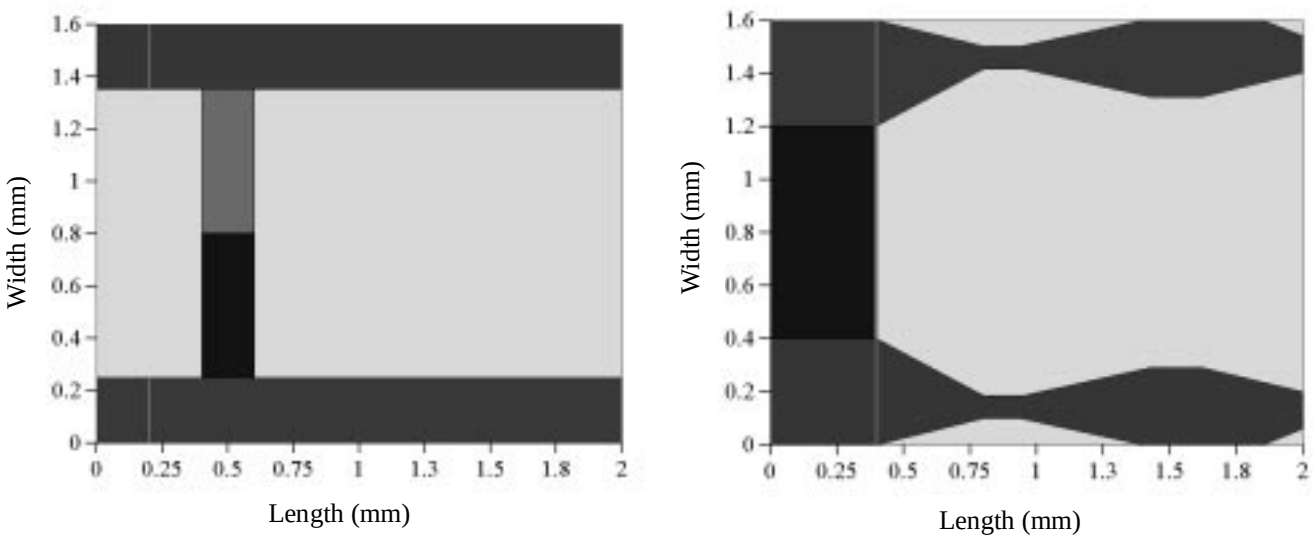

(a) TFN slider

(b) Headway_AAB slider

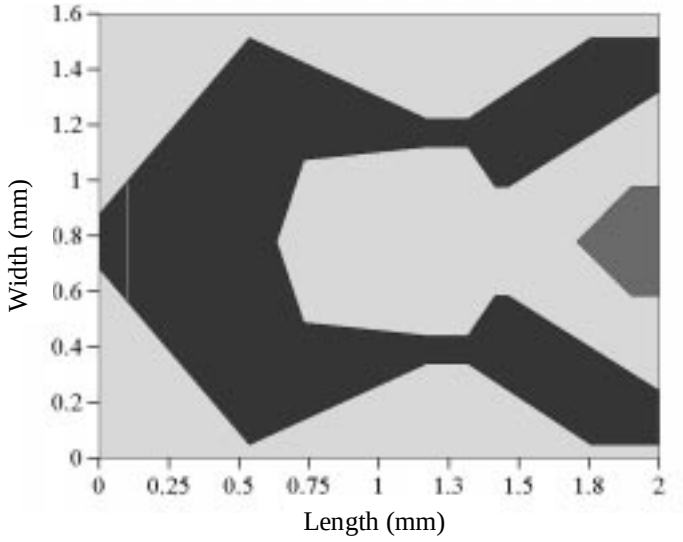

(a) NSIC “Nutcracker” slider

Fig. 1 Air Bearing Surface for the Positive

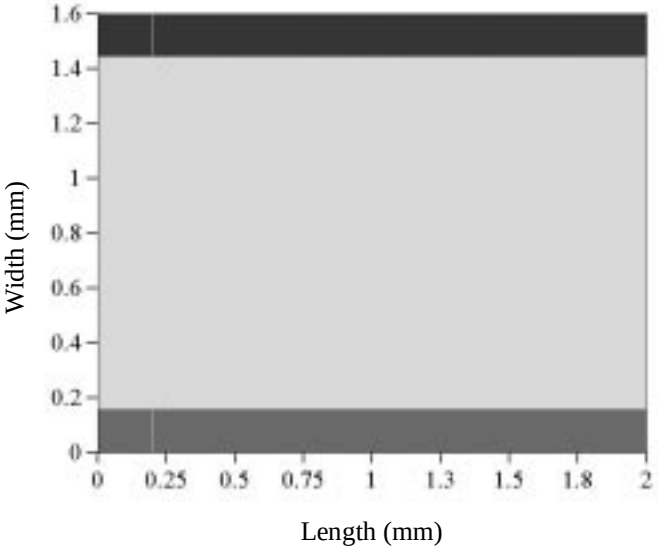

(a) TF Slider

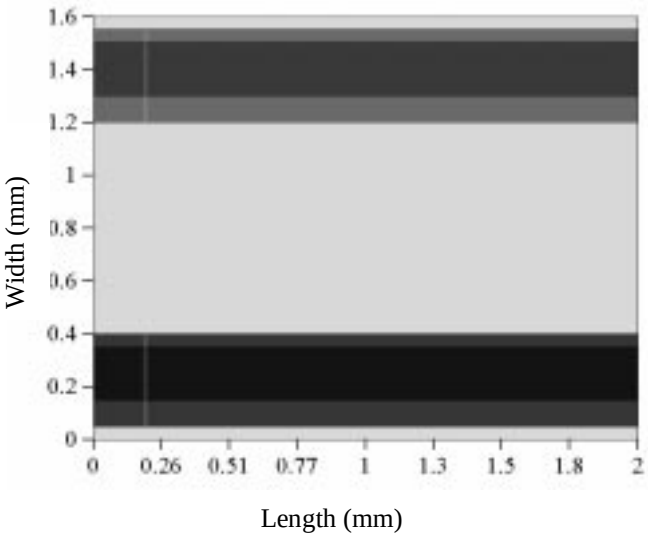

(b) TPC Slider

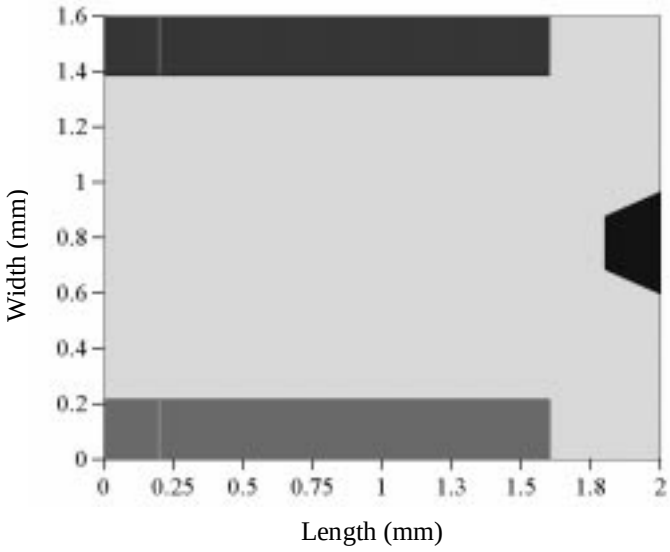

(c) Tri-Pad Slider

Fig. 2 Air Bearing Surface for the Positive

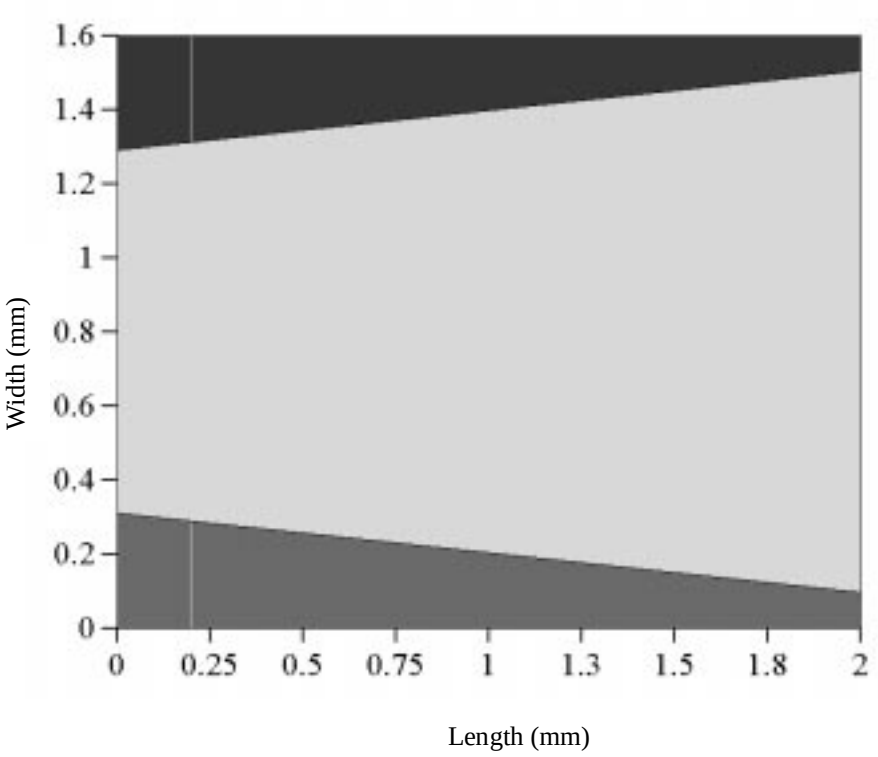

Fig. 2 Air Bearing Surface for the modified TF slider

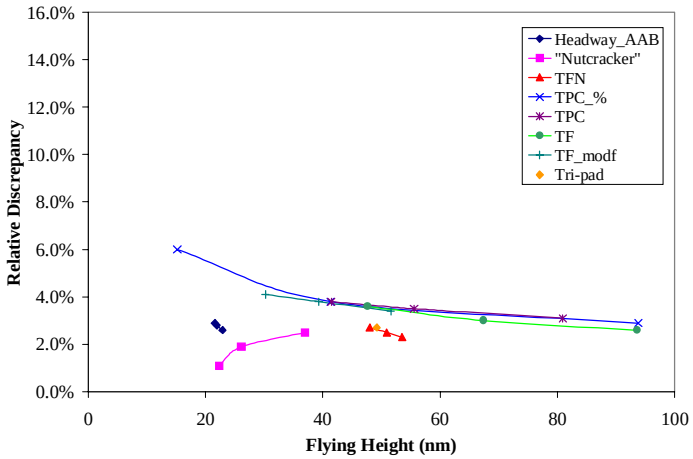

(a)

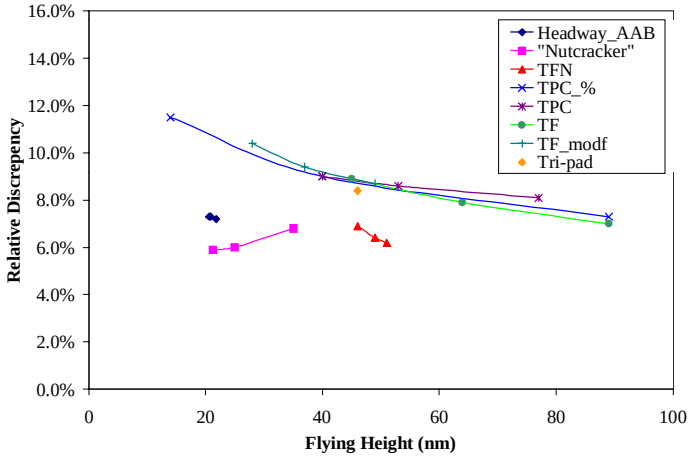

(b)

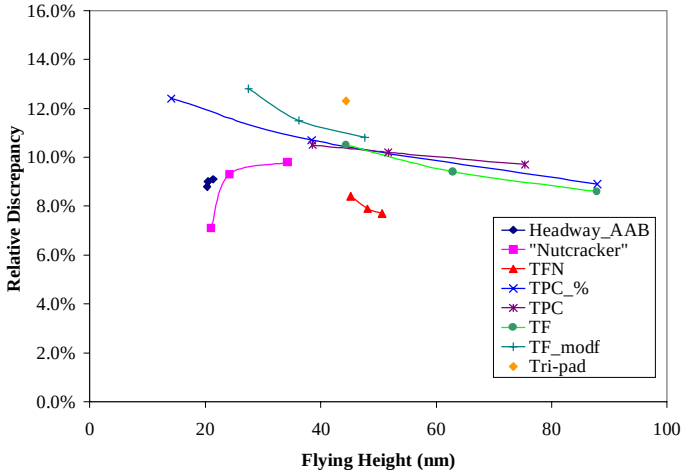

(c)

Fig 4. Relative Discrepancy of the Flying Height vs. Flying Height
(a) $\alpha_0 = 0.95$, $\alpha_1 = 1$ (b) $\alpha_0 = 0.90$, $\alpha_1 = 0.95$ (c) $\alpha_0 = 0.90$, $\alpha_1 = 0.90$